Electronic Supplementary Material (ESI) for New Journal of Chemistry.

Supplementary Information

Photocatalytic dehydrogenation of ammonia borane over Ti_3C_2/MOF-supported Pd-doped Co nanoparticles

Xiaodie Huang, Ziye Liu, Jingjing Tu, Changchun Ji, Ying-Hua Zhou*

The Key Laboratory of Functional Molecular Solids, Ministry of Education, Anhui Laboratory of Molecule-Based Materials (State Key Laboratory Cultivation Base), College of Chemistry and Materials Science, Anhui Normal University, Wuhu, Anhui 241002, China

E-mail: yhzhou@ahnu.edu.cn

Table S1 ICP-OES results of the refresh and used $Co_{30}Pd$@TUNS.

	Pd (wt%)	Co (wt%)	n_{Co} : n_{Pd}
the refresh	0.2724	4.6835	~30 :1
the used	0.2514	4.4521	~30 :1

Table S2 The calculated XPS elemental compositions in Ti_3C_2, TUNS and $Co_{30}Pd$@TUNS

Elemental atomic %	Ti_3C_2	TUNS	$Co_{30}Pd$@TUNS
C1s	45.39	41.41	45.83
Ti2p	30.69	4.16	2.27
O1s	23.91	45.11	41.29
Zr3d	-	4.25	2.89
N1s	-	5.07	1.92
Co2p	-	-	5.73
Pd3d5	-	-	0.05

Table S3 Turnover frequency (TOF) and activation energy (E_a) values of Co-based catalysts for dehydrogenation of ammonia borane at 298 K.

Catalyst	TOF ($mol_{H2}·mol_{metal}^{-1}·min^{-1}$)	E_a ($kJ·mol^{-1}$)	Ref.
Co/PEI-GO [a]	39.9	28.2	[S1]
Co/MXene	12.5	33.05	[S2]
$Cu_{0.8}Co_{0.2}O$/GO	70.0	45.53	[S3]
rGO-$Co_{70}Ru_{30}$	95.0	55.6	[S4]
RuCo(1:1)/g-Al_2O_3	35.9 [b]	47.0	[S5]
$Cu_{0.72}Co_{0.18}Mo_{0.1}$	119.0	45.0	[S6]
Co/PCN	82.04	-	[S7]
AuCo/NCX-1	42.1	31.92	[S8]
CuCo@MIL-101	19.6	-	[S9]
CoPd/C	27.7 [c]	27.5	[S10]
CoRh@PVP	154	42.7	[S11]
Ru@Co/CCF	139.59 [c]	57.02	[S12]
CoCu-BCs/GO	72.4	47.8	[S13]
Co_4N-Co_3O_4@C	79.0	28.8	[S14]
CoP-CoO/NCDs	89.6	41	[S15]
ZIF-67@Co	112.3	-	[S16]
$Co_{0.7}Ni_{0.3}$	35.3	23.6	[S17]
Co@$Co_2Mo_3O_8$	17.3	51.8	[S18]
$CuCo_2O_4$	104.0	22.6	[S19]
$Cu_{0.5}$@$Co_{0.5}$-MOF/5	130.0	26.5	[S20]
Co/C_3N_4-540	83.3	-	[S21]
Cu@Co/rGO	8.7	51.3	[S22]
Co_{30}Pd@TUNS	130.37	25.8	this work

[a] GO = graphene oxide;

[b] TOF value is obtained at 323 K;

[c] TOF value is obtained at 303 K.

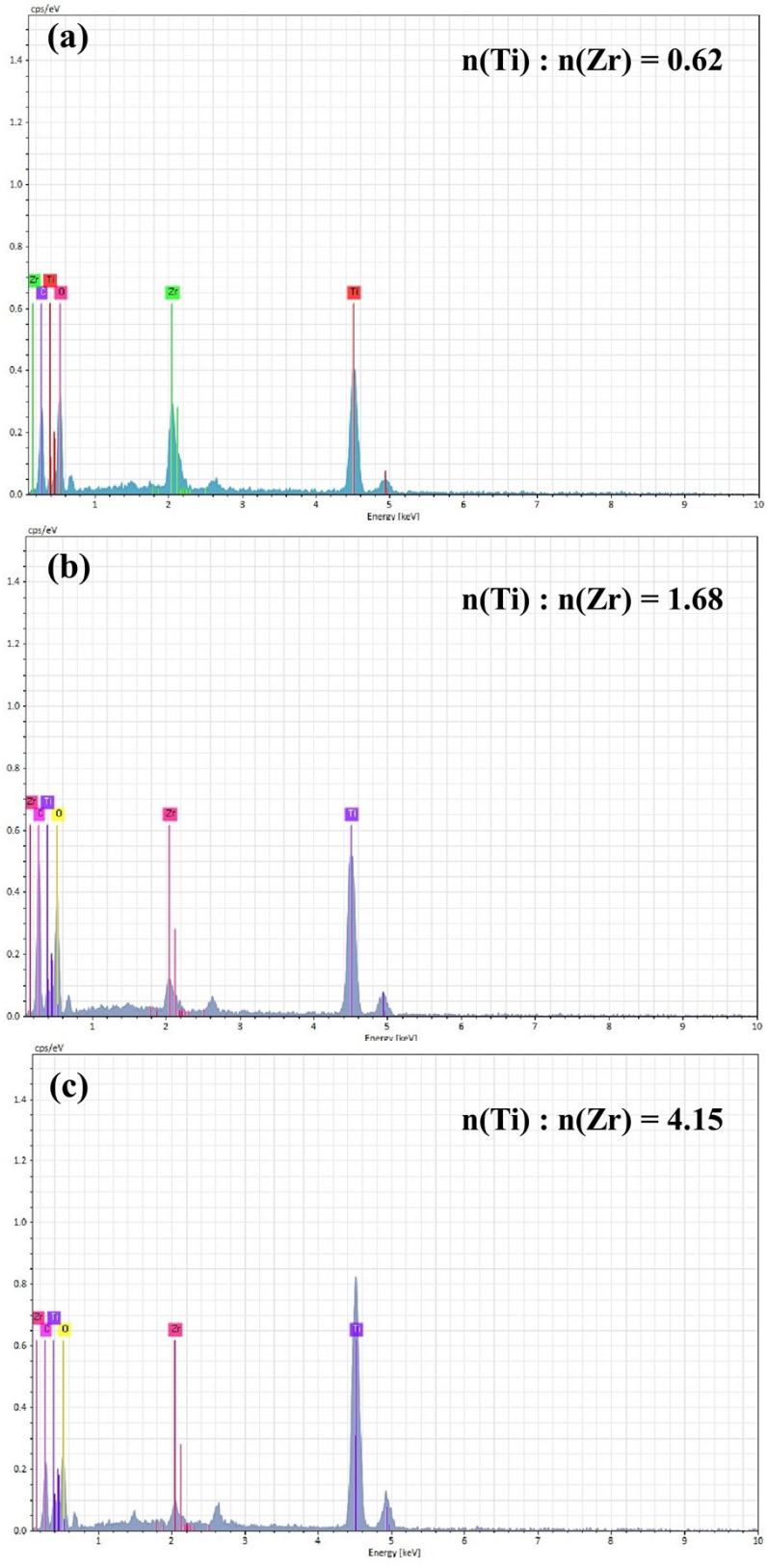

Fig. S1 EDS patterns of composites with different ratios of Ti_3C_2 to UiO-66-NH_2. (a) TUNS-*l*, (b) TUNS, and (c) TUNS-*m*.

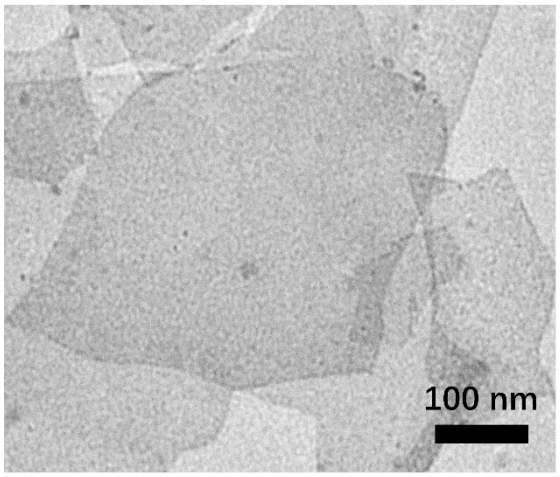

Fig. S2 TEM image of Ti_3C_2 nanosheets.

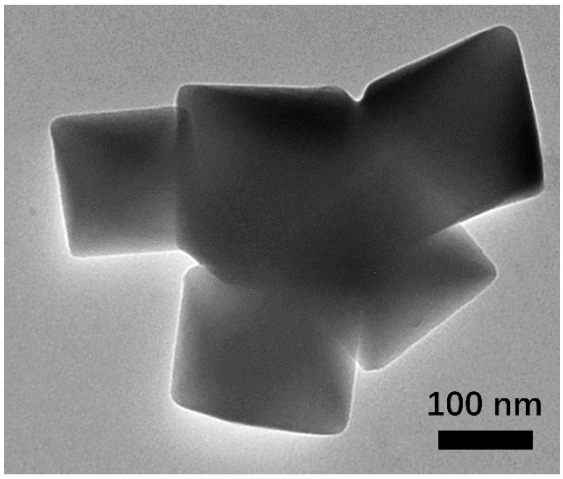

Fig. S3 TEM image of UiO-66-NH_2.

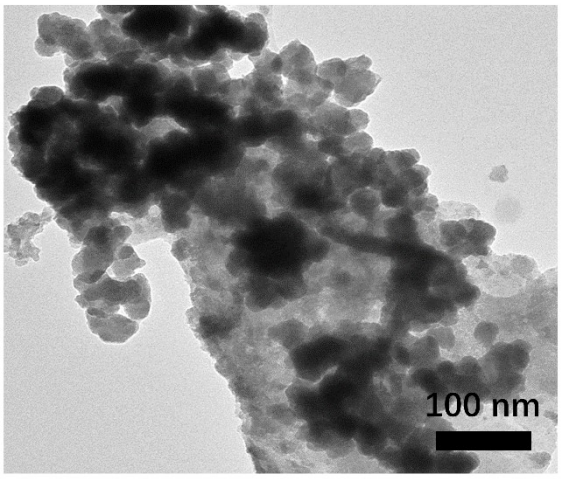

Fig. S4 TEM image of TUNS.

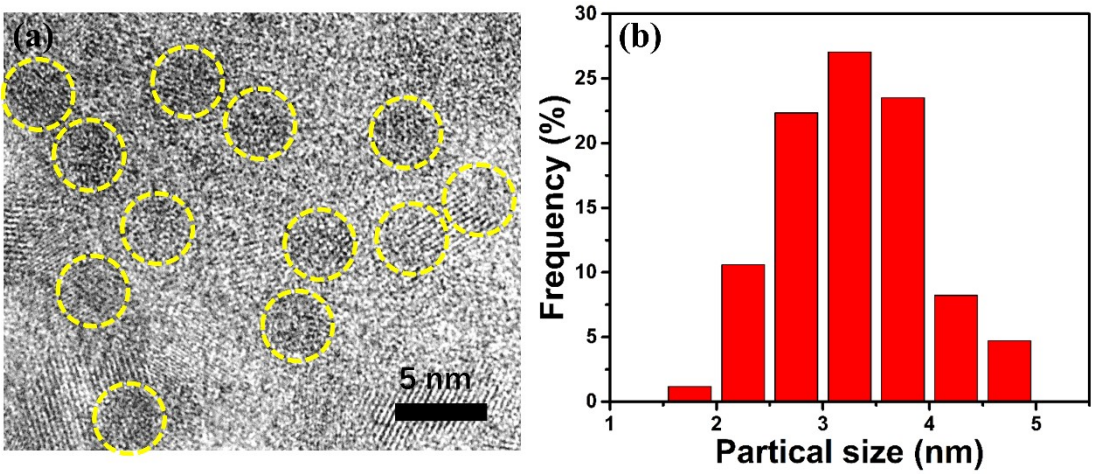

Fig. S5 (a) HRTEM image, and (b) metal NPs size-distribution histogram of $Co_{30}Pd$@TUNS.

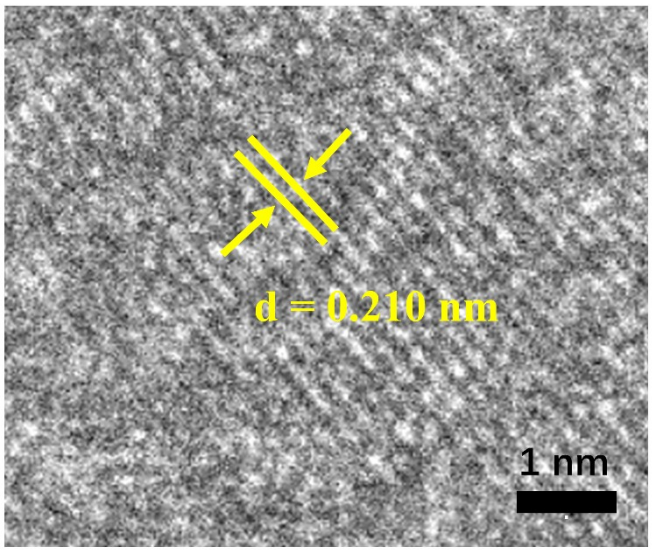

Fig. S6 HRTEM image of $Co_{30}Pd$@TUNS.

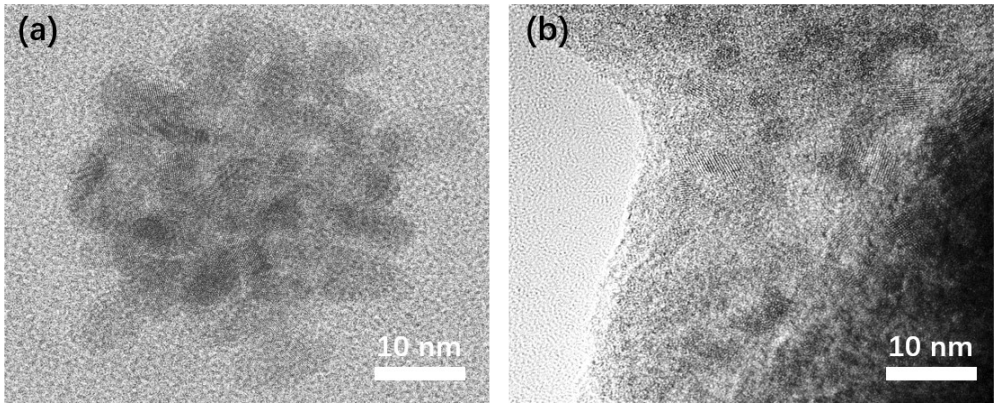

Fig. S7 HRTEM image of (a) $Co_{30}Pd$/TUNS and (b) $Co_{30}Pd$@TUNS.

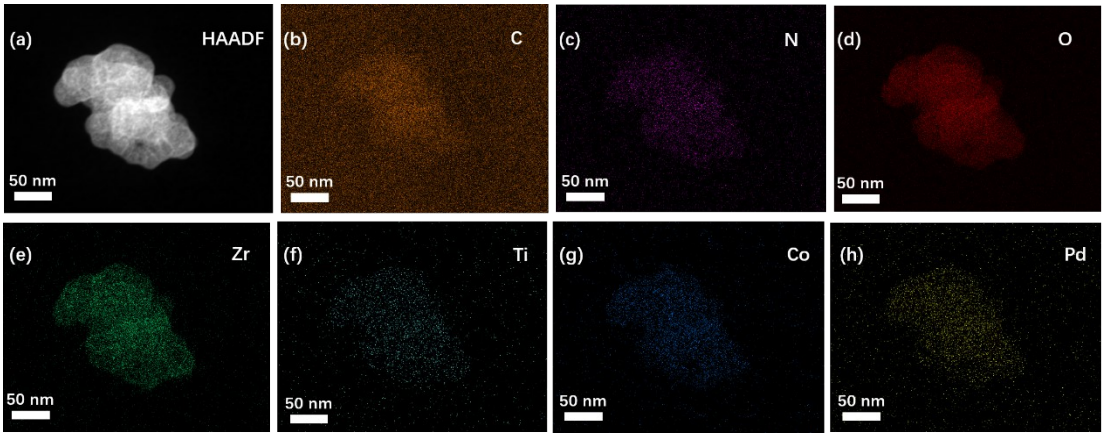

Fig. S8 Elemental mappings of $Co_{30}Pd$@TUNS.

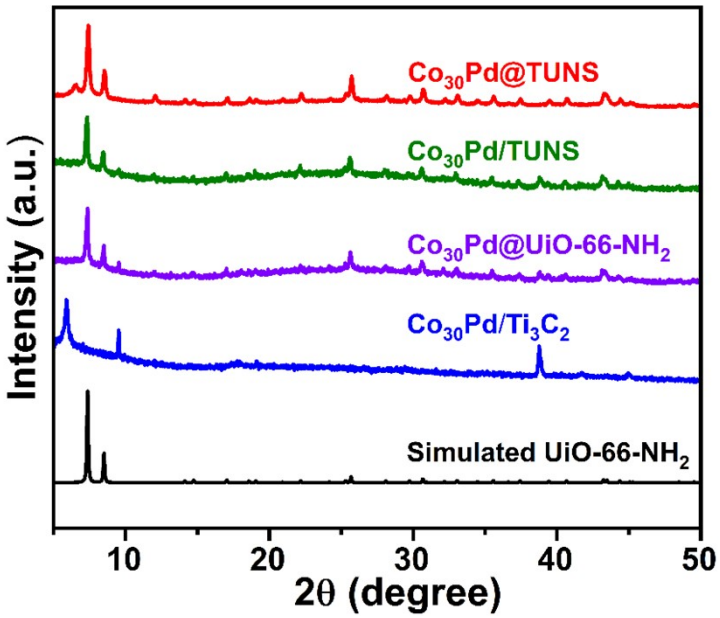

Fig. S9 PXRD patterns of the as-synthesized samples with different support.

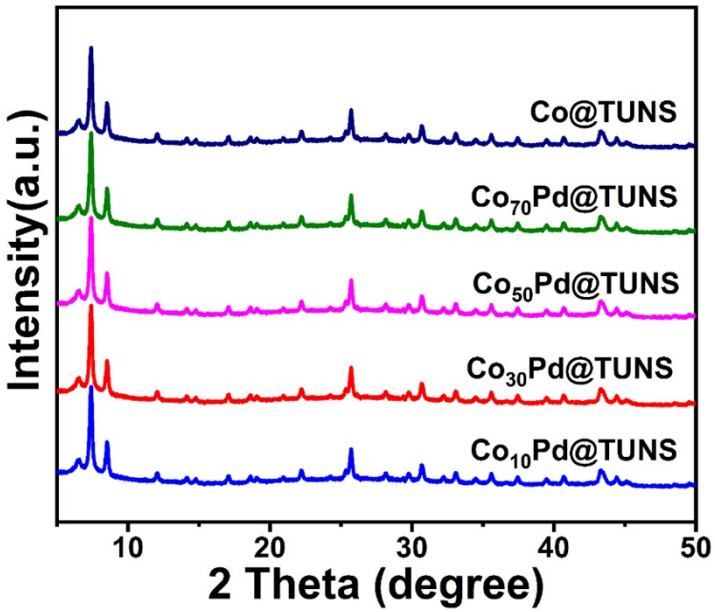

Fig. S10 PXRD patterns of the as-synthesized samples with various ratios of Pd and Co.

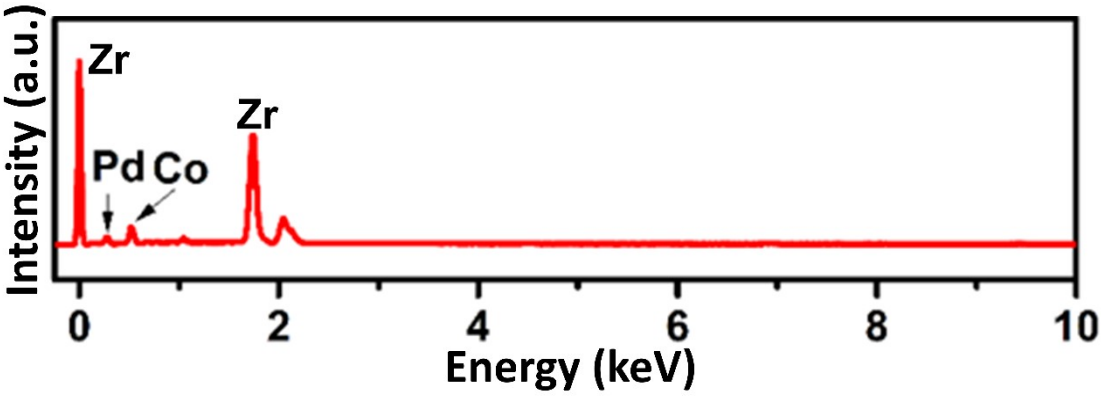

Fig. S11 EDS patterns of $Co_{30}Pd$@TUNS.

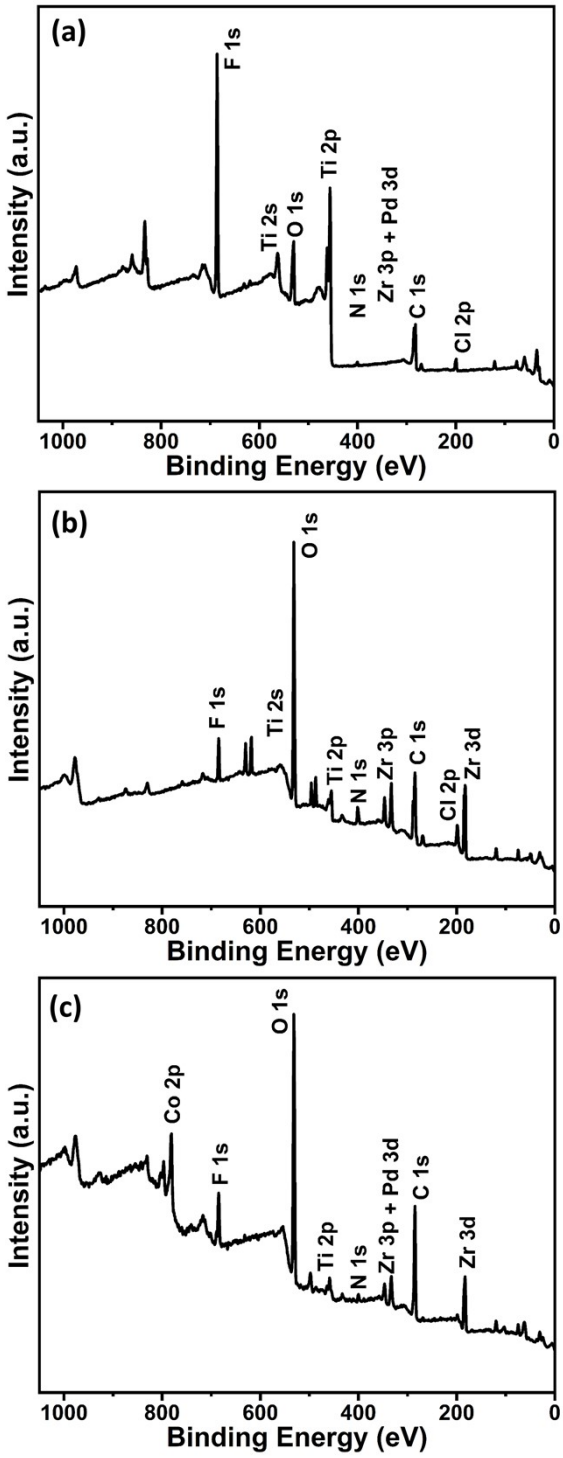

Fig. S12 XPS survey spectrum of (a) Ti_3C_2, (b) TUNS, and (c) $Co_{30}Pd$@TUNS.

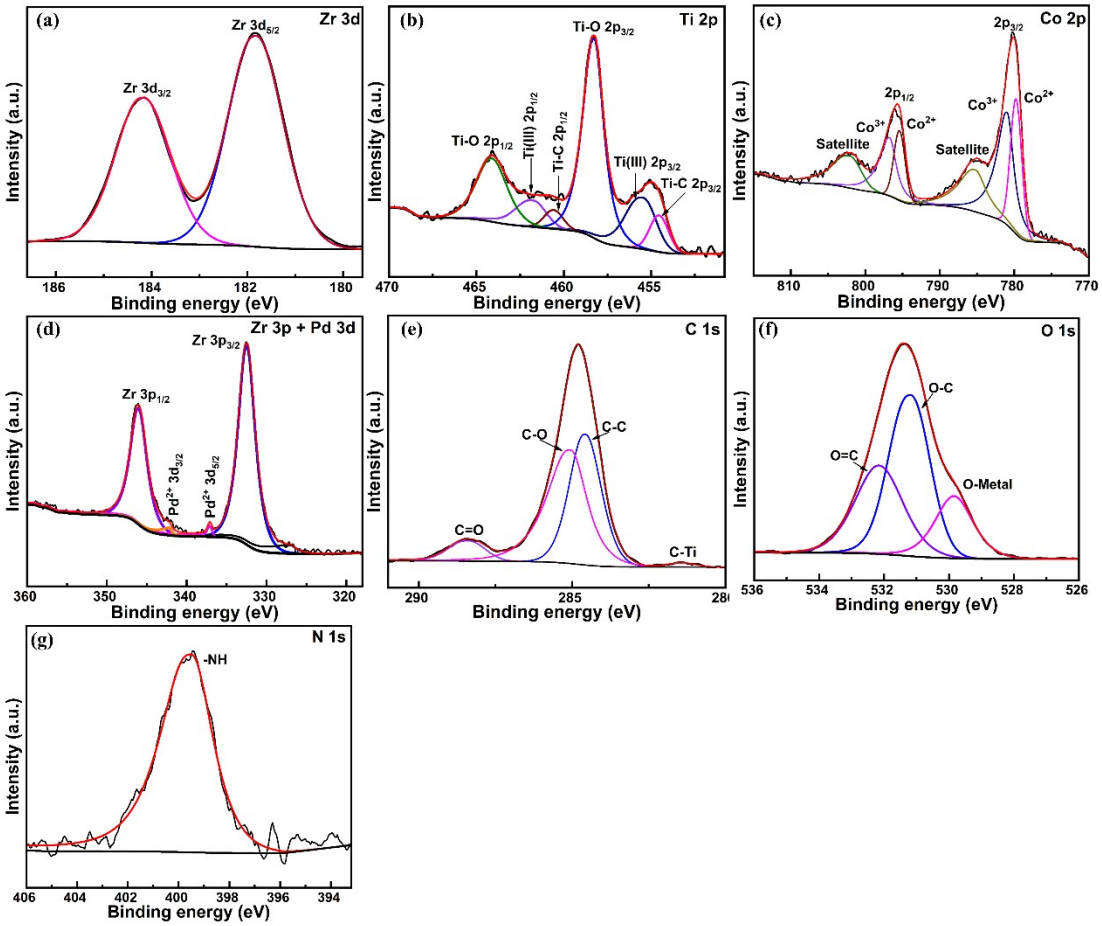

Fig. S13 The high-resolution XPS spectra of $Co_{30}Pd$@TUNS (a) Zr 3d, (b) Ti 2p, (c) Co 2p, (d) Zr 3d + Pd 3d, (e) C 1s, (f) O 1s, and (g) N 1s.

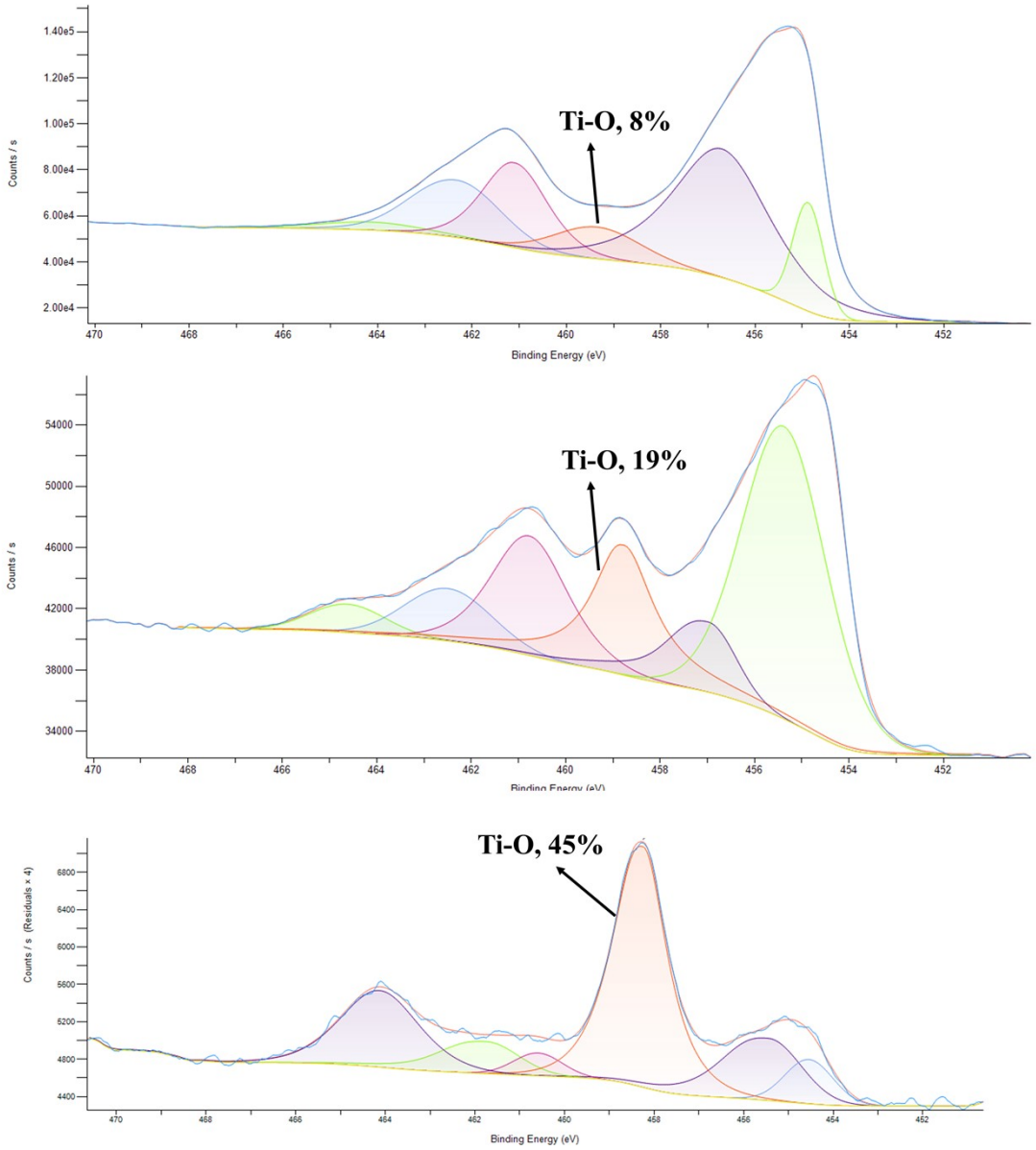

Fig. S14 The high-resolution XPS spectra of Ti 2p in (a) Ti_3C_2, (b) TUNS, and (c) $Co_{30}Pd$@TUNS. Note: the Ti-O concentration was estimated by calculating the area ratio of this peak to all peaks.

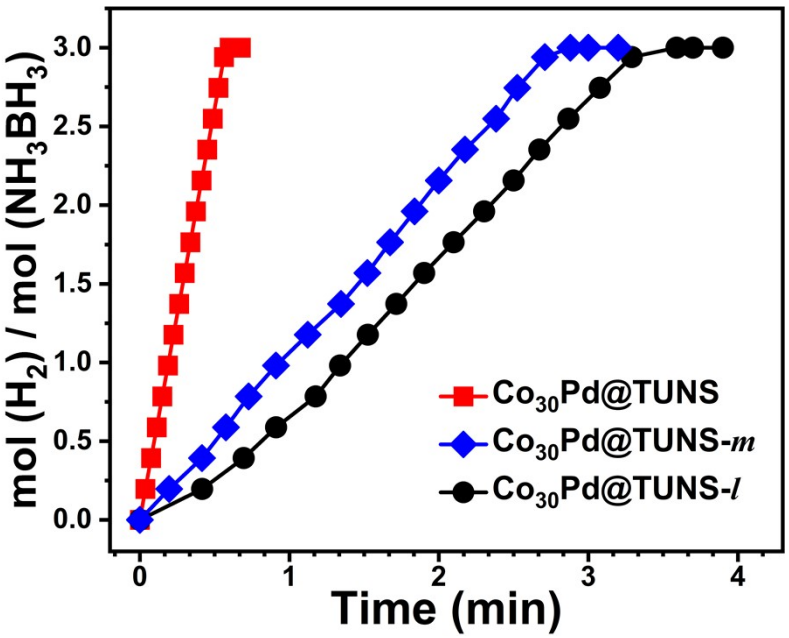

Fig. S15 Time courses for hydrogen production from AB over catalyst under the light irradiation of 300 W Xe lamp at 298 K.

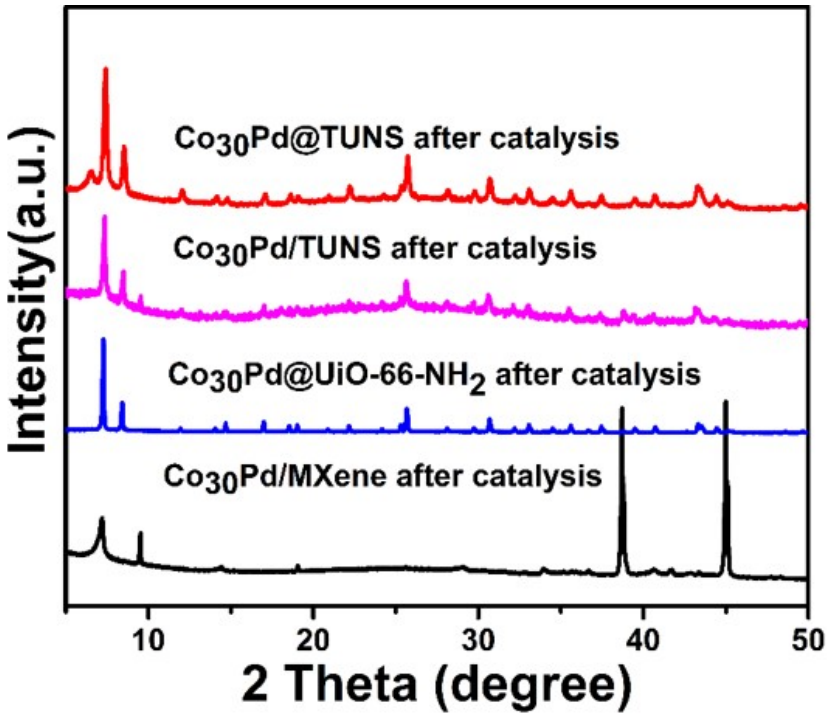

Fig. S16 XRD patterns of the composites after catalysis.

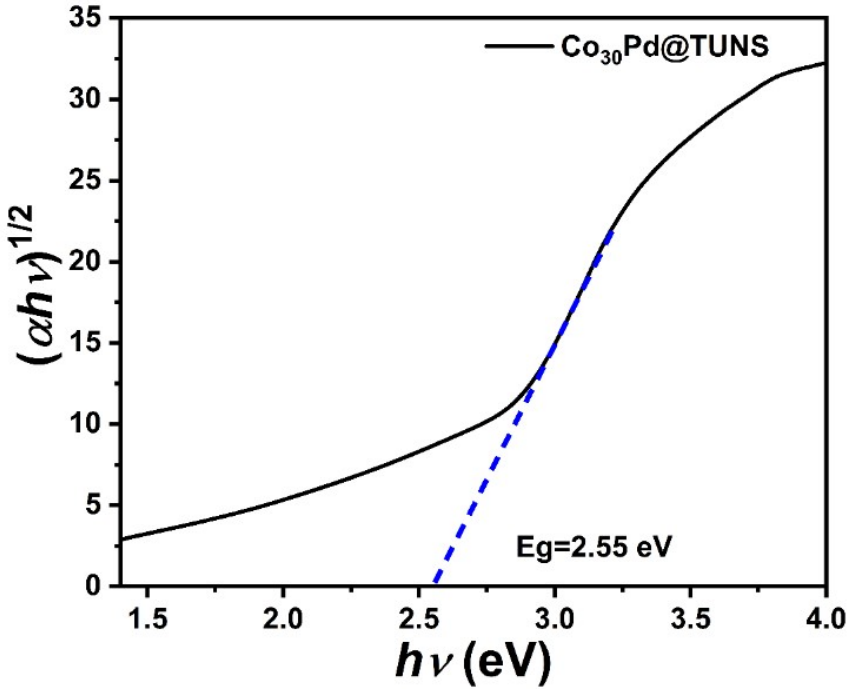

Fig. S17 The Tauc plot of $Co_{30}Pd$@TUNS. The plot has a steep region, in which the linear increase of light absorption with increasing energy. The band gap energy is deduced by the *x*-axis intersection point of the linear fitting according to the equation of $(\alpha h\nu)^{1/2} = B(h\nu - E_g)$, where α refers to the absorption coefficient of the material, *B* is a constant, *h* is the Planck constant, *v* is the photon's frequency, and E_g is the band gap energy.

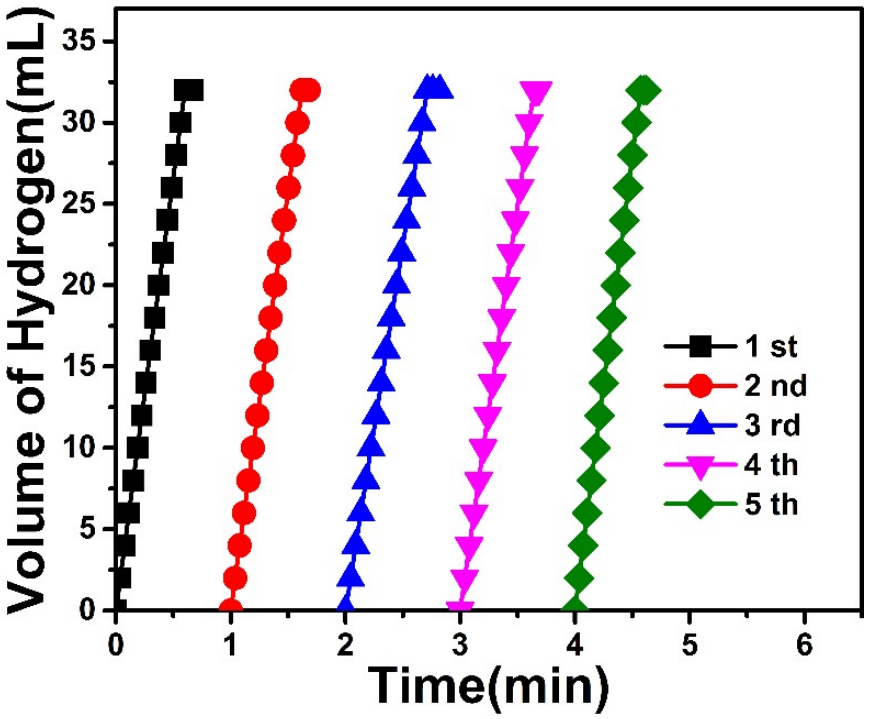

Fig. S18 Recyclability test for AB (15.5 mg) dehydrogenation over $Co_{30}Pd$@TUNS (15 mg) under the irradiation of 300 W Xe lamp.

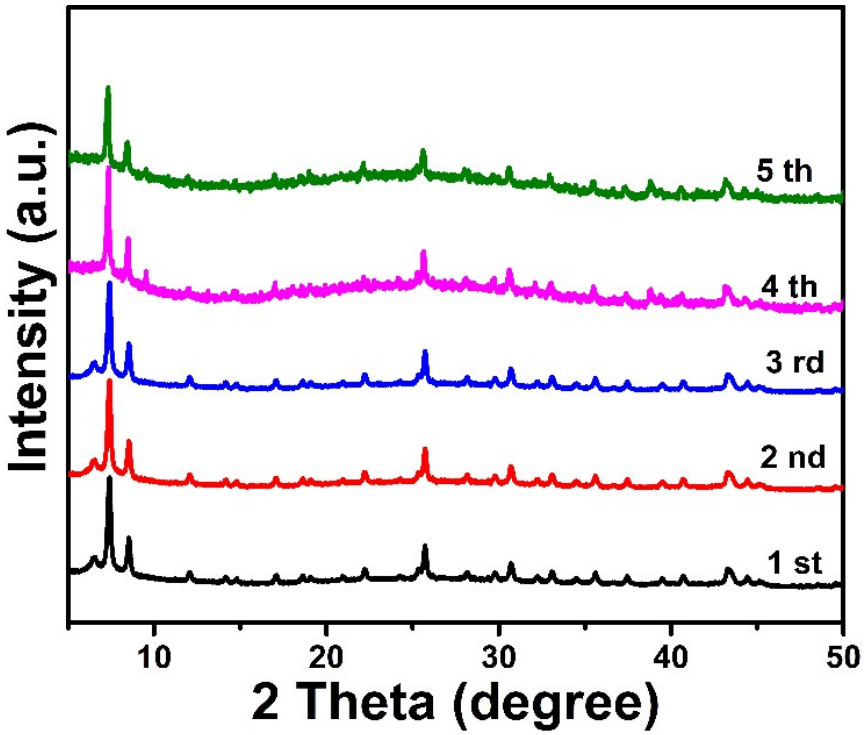

Fig. S19 XRD patterns of $Co_{30}Pd$@TUNS after five cycles.

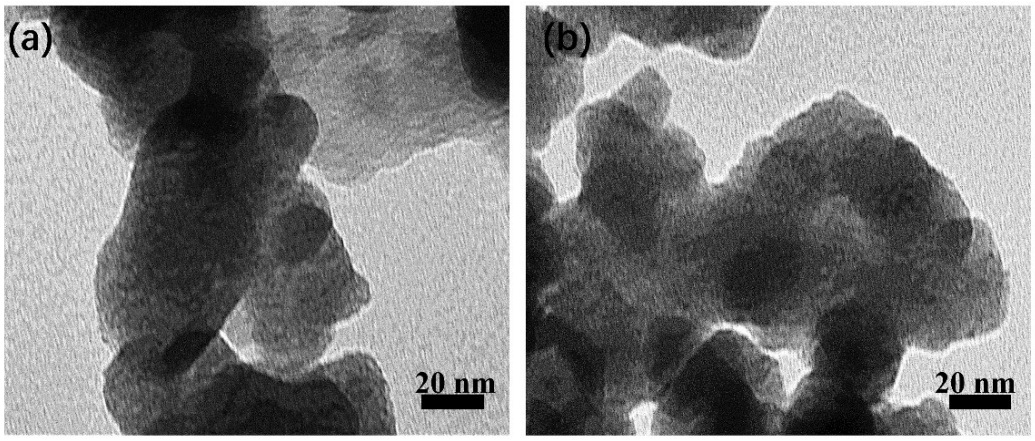

Fig. S20 TEM image of $Co_{30}Pd$@TUNS (a) before first run, and (b) after fifth run.

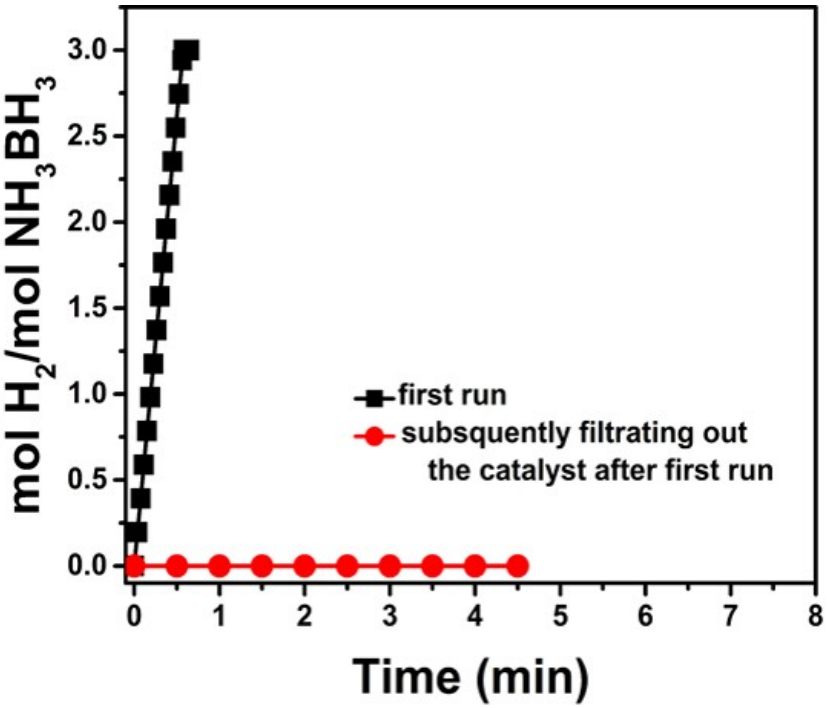

Fig. S21 Plots of time versus conversion of hydrogen generation from ammonia borane catalyzed by filtrating out $Co_{30}Pd$@TUNS catalyst after the first run at 298 K.

References

[S1] Hu J, Chen Z, Li M, Zhou X, Lu H. *ACS Appl Mater Interfaces* 2014;*6*:13191.

[S2] Liu T, Wang QT, Sun YH, Zhao M. J Nanosci *Nanotechnol* 2019;*19*:7392.

[S3] Feng K, Zhong J, Zhao B, Zhang H, Xu L, Sun X, et al. *Angew Chem Int Ed* 2016;*55*:11950.

[S4] Can H, Can S, Ebiri R, Metin Ö. *New J Chem* 2022;*46*:12120-31.

[S5] Rachiero GP, Demirci UB, Miele P. *Int J Hydrogen Energy* 2011;*36*:7051-65.

[S6] Yao Q, Yang K, Hong X, Chen X, Lu ZH. *Catal Sci Technol* 2018;*8*:870-7.

[S7] Zhang S, Xu J, Cheng H, Zang C, Bian F, Sun B, et al. *ChemSusChem* 2020;*13*:5264-72.

[S8] Guo L, Gu X, Kang K, Wu Y, Cheng J, Liu P, et al. *J Mater Chem* 2015;*3*:22807-15.

[S9] Li J, Zhu QL, Xu Q. Catal Sci Technol 2015;5:525-30.

[S10] Sun D, Mazumder V, Metin Ö, Sun S. *ACS Nano* 2011;*5*:6458-64.

[S11] Rakap M. *Renew Energ* 2020;*154*:1076-82.

[S12] Yang J, Cui Z, Ma J, Dong Z. *Int J Hydrogen Energy* 2018;*43*:1355-64.

[S13] Y. Chen, K.Wang, K. Nie, J.Wang, S.Wang, K. Feng, J. Zhong, *Chem. Eng. J.* 2023, *451*, 138931.

[S14] S. Guan, Y. Liu, H. Zhang, H. Wei, T. Liu, X. Wu, H. Wen, R. Shen, S. Mehdi, X. Ge, C. Wang, B. Liu, E. Liang, Y. Fan, B. Li, *Small* 2022, *18*, 2107417.

[S15] H. Wu, Y. Cheng, B. Wang, Y. Wang, M. Wu, W. Li, B. Liu, S. Lu, *J. Energy Chem.* 2021, *57*, 198.

[S16] W. Wang, M. Liang, Y. Jiang, C. Liao, Q. Long, X. Lai, L. Liao, *Mater. Lett.* 2021, *293*, 129702.

[S17] X. Su, S. Li, *Int. J. Hydrogen Energy* 2021, *46*, 14384.

[S18] J. He, Z. Huang, W. Chen, X. Xiao, Z. Yao, Z. Liang, L. Zhan, L. Lv, J. Qi, X. Fan, L. Chen, *Chem. Eng. J.* 2021, *431*, 133697.

[S19] Y. Feng, J. Liao, X. Chen, H. Wang, B. Guo, H. Li, L. Zhou, J. Huang, H. Li, *J. Alloys Compd.* 2021, *863*, 158089.

[S20] W. Xu, W. Li, H. Wen, J. Ding, Y. Liu, W. Li, B. Li, *Appl. Catal., B* 2021, *286*, 119946.

[S21] H. Zhang, X. Gu, J. Song, N. Fan, H. Su, *ACS Appl. Mater. Interfaces* 2017, *9*, 32767.

[S22] Y. Du, N. Cao, L. Yang, W. Luo, G. Cheng, *New J. Chem.* 2013, *37*, 3035.